ELSEVIER

Catalysis Today 26 (1995) 239–245

CATALYSIS TODAY

Catalytic properties and surface modification of hexaaluminate microcrystals for combustion catalyst

M. Machida [a,*], A. Sato [a], T. Kijima [a], H. Inoue [b], K. Eguchi [b], H. Arai [b]

[a] *Department of Materials Science, Faculty of Engineering, Miyazaki University, Gakuen Kibanadai Nishi 1-1, Miyazaki 889-21, Japan*

[b] *Department of Materials Science and Technology, Graduate School of Engineering Sciences, Kyushu University, Kasugakoen 6-1, Kasuga, Fukuoka 816, Japan*

Abstract

Spinel oxide (Mn_3O_4) surface layers were produced on hexaaluminate microcrystals by means of the air-oxidation process. The surface layer completely covered the basal plane of hexagonal facets as evident from HREM observation and CO_2 chemisorption measurement. The catalytic activity of as prepared Mn_3O_4/hexaaluminate composites for methane combustion was evaluated as functions of the Mn_3O_4 loading and the metal composition of the spinel surface layer. It was revealed that the air oxidation-derived composites showed the excellent specific activities superior to those of the corresponding Mn_3O_4/hexaaluminates prepared from the conventional evaporation-to-dryness process. Partial substitution of Fe for Mn of the surface layer was effective in enhancing combustion activity in a whole temperature range.

Keywords: Surface modification; Hexaaluminate microcrystals; Combustion

---

1. Crystallographic analysis on thermal stability and catalytic property of hexaaluminates

1.1. *Crystallographic consideration on retention of large surface area*

Hexaaluminate-related compounds are eminently suitable for a high-temperature combustion catalyst not only because of the excellent thermal stability but also because of the high catalytic activity for methane combustion. We noticed the relation between these useful functions and the unique layer crystal structure of this compound, which consists of the alternative stacking of a spinel block and a monatomic layer including large cations such as Ba or La (Fig. 1). We conducted various crystallographic analyses on single crystal- as well as polycrystalline-hexaaluminates to elucidate these characteristic functions as summarized schematically in Fig. 1. The thermal stability of hexaaluminate is reflected by the retention of large specific surface area (> 20 m^2/g) even at high temperatures (> 1200°C) [1–4]. The retention of the large surface area is closely related to the very thin planar morphology of hexaaluminate microcrystals. From the grain growth rate analysis, the crystal growth along [001], being suppressed strongly [5], is a reason of the planar morphology. The basic interpretation between the layer structure, sintering, and grain growth requires information about solid state oxide-ions diffusion, because, in many cases, the

---

* Corresponding author.

SSDI 0920-5861(95)00145-X

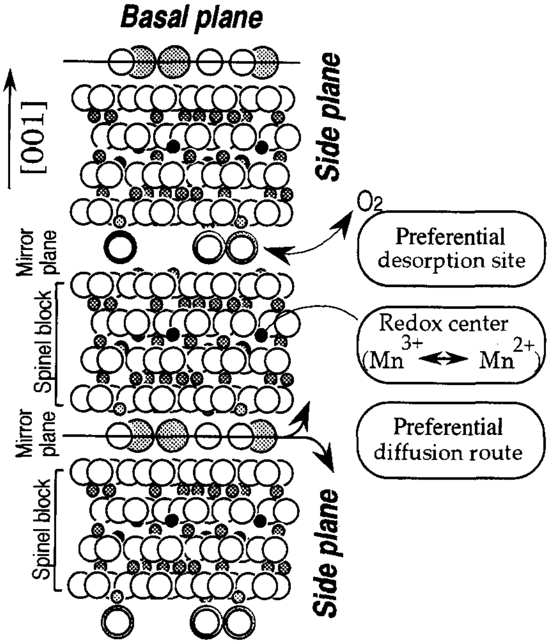

Fig. 1. Crystal structure and morphology of powder samples of Mn-substituted hexaaluminate (BMA).

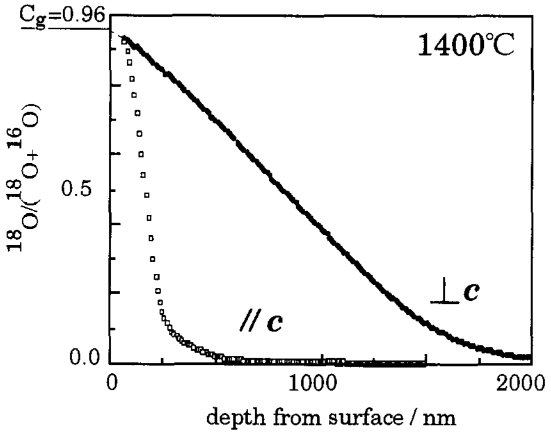

Fig. 2. Depth profiles of ^{18}O concentration in Ba-hexaaluminate single crystal after the isotope exchange at 1400°C. Isotope exchange: $C_g=0.96$, $t=7200$ s, O_2 pressure = 2 kPa, SIMS: Cs^+, 10 keV, 20 nA. $D_{\perp c}$, $9.35\cdot10^{-13}\ \mathrm{cm^2/s}$; $D_{\parallel c}$, $2.59\cdot10^{-14}\ \mathrm{cm^2/s}$.

oxide ions are the slowest species in metal oxides and influence the sintering rate. Secondary-ion mass spectrometric analysis (SIMS) of isotopic oxygen self-diffusion in the single crystal indicated that diffusivities (D) of oxide ion normal to c axis ($_\perp c$) was an order of magnitude larger than those along c axis ($_\parallel c$) as shown in Fig. 2. This suggests that some preferential diffusion route with a lower activation energy lie in the $_\perp c$ direction. In the hexaaluminate structure, an oxygen close-packed part (spinel block) is fold together by the loosely packed monolayer (mirror plane). Since the ideal density of oxygen of the mirror plane is only a quarter of that in spinel blocks, it is reasonable that the mirror plane is a preferential diffusion route of oxygen. As a result of anisotropic diffusion in the mirror plane, which promotes the transfer of constitute ions from bulk to surface, preferential grain growth of hexaaluminate along the $_\perp c$ direction seems to take place [6–8]. However, since such thin particles with the large aspect ratio must be unstable because of increased surface energy, the particle size does not increase easily at elevated temperatures.

1.2. Crystallographic consideration on the catalytic activity

The Al sites in hexaaluminate can be partially replaced by transition elements. The catalytic activity of cation substituted hexaaluminate is related to the reduction/oxidation behavior of transition elements in the crystal lattice. The reduction/oxidation of manganese, which is reversible between di- and trivalent states in the hexaaluminate lattice, leads to high catalytic activity for methane combustion. The SIMS analysis for isotopic exchange of oxygen also implied

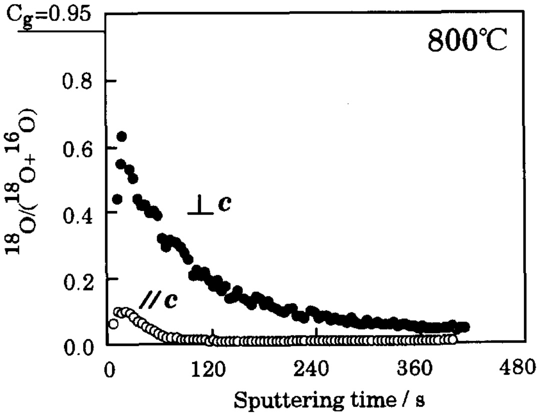

Fig. 3. Depth profiles of ^{18}O concentration near surface of Mn-substituted hexaaluminate single crystal after the isotope exchange at 800°C. Isotope exchange: $C_g=0.95$, $t=7200$ s, O_2 pressure = 2 kPa, SIMS: Cs^+, 5 keV, 50 nA. k_{hk0}, $3\cdot10^{-11}$ cm/s; k_{00l}, $1\cdot10^{-12}$ cm/s.

that the rate of isotopic surface exchange strongly depends on the exposed crystal plane of the Mn-substituted hexaaluminate single crystal. Fig. 3 shows the typical concentration profiles of ^{18}O in Mn-substituted hexaaluminate in $_{\parallel}c$ and $_{\perp}c$ directions. It is apparent that ^{18}O penetration along [110] was more significant than along [001] because of the anisotropic oxygen diffusion. In this case, however, the surface concentration of ^{18}O was smaller than the concentration in the gas phase (C_g). This means that the ^{18}O transfer from gas phase to Mn-substituted hexaaluminate was controlled not only by bulk diffusion but also by an isotopic exchange reaction at each surface. The (110) surface shows a catalytic activity for isotopic exchange reaction (k) higher than that of the (001) surface. From this result, it is deduced that the higher catalytic activity is attained on the side plane ($_{\parallel}c$) of the hexaaluminate microcrystal rather than on the basal plane ($_{\perp}c$) of the facet. From this anisotropic surface exchange rate, it is clear that the catalytic activity is also influenced by the layer structure.

In this regard, the study was directed towards structural analysis of the Mn-substituted hexaaluminate single crystal as grown in air and after subsequent reduction by means of evacuation at 1150°C. Table 1 and Table 2 represent the result of X-ray structural analysis. The results suggest that, after reduction treatment, the occupancies of mirror plane oxygen sites, O(5), O(6), O(7), decreased whereas the those of oxygen inside spinel blocks, O(1)–O(4), remained unchanged. During reduction, tetrahedrally-coordinated Mn^{3+} in spinel blocks was partially reduced to Mn^{2+} as confirmed by electron spectroscopic analysis. Consequently, mirror plane oxygen sites preferentially participate in the sorption/desorption accompanied by oxidation/reduction of Mn species in the hexaaluminate structure. As can be seen in Fig. 1, the presence of such preferential oxygen sites led to the higher catalytic activity of crystal surface corresponding to side planes of hexagonal facet ($_{\parallel}c$). This is in consistent with the anisotropic surface exchange rate of Mn-substituted hexaaluminate (Fig. 3)

Table 1
Structural parameters of as-grown BMA

Atom	Position	x	z	Occupancy
Ba	6(h)	2/3	1/4	0.0650
Mn	4(f)	1/3	0.0237	0.0212
Al(1)	12(k)	0.83309	0.10528	0.4702
Al(2)	4(f)	1/3	0.02374	0.1455
Al(3)	4(f)	1/3	0.17512	0.1667
Al(4)	2(a)	0	0	0.0833
Al(5)	12(k)	0.840	0.1774	0.0265
O(1)	12(k)	0.1568	0.05013	0.5000
O(2)	12(k)	0.5039	0.14734	0.5000
O(3)	4(f)	2/3	0.05676	0.1667
O(4)	4(e)	0	0.14207	0.1667
O(5)	2(c)	1/3	1/4	0.0196
O(6)	6(h)	0.2949	1/4	0.0667
O(7)	6(h)	0.880	1/4	0.0097

$R=0.029$, $R_w=0.039$, calculated composition: $Ba_{0.78}Mn_{0.25}Al_{10.71}O_{17.15}$. $P6_3/mmc$, $a=0.5591$ nm, $c=2.2659$ nm.

Table 2
Structural parameters of BMA after reduction

Atom	Position	x	z	Occupancy
Ba	6(h)	2/3	1/4	0.0655
Mn	4(f)	1/3	0.02373	0.0198
Al(1)	12(k)	0.83308	0.10520	0.4680
Al(2)	4(f)	1/3	0.02373	0.1469
Al(3)	4(f)	1/3	0.17517	0.1667
Al(4)	2(a)	0	0	0.0833
Al(5)	12(k)	0.8408	0.1770	0.0272
O(1)	12(k)	0.15672	0.05013	0.5000
O(2)	12(k)	0.50401	0.14733	0.5000
O(3)	4(f)	2/3	0.05660	0.1667
O(4)	4(e)	0	0.14218	0.1667
O(5)	2(c)	1/3	1/4	0.0191
O(6)	6(h)	0.2943	1/4	0.0653
O(7)	6(h)	0.881	1/4	0.0089

$R=0.026$, $R_w=0.033$, calculated composition: $Ba_{0.79}Mn_{0.24}Al_{10.71}O_{17.12}$. $P6_3/mmc$, $a=0.5587$ nm, $c=2.2656$ nm. O(1)–O(4): close-packed O^{2-} inside spinel blocks; O(5)–O(7): mirror plane O^{2-} between spinel blocks.

2. Surface modification of hexaaluminate microcrystals

As summarized briefly in the preceding section, the basal plane of hexaaluminate facet seems less active than the side plane. Thus, the following study was directed toward the surface modification of hexaaluminate microcrystals in order to enhance the catalytic activity. Fortunately, the flat surface of the basal plane must be suitable for a substrate for the crystal growth of other oxide layers. The resultant composite microcrystals are expected to produce interesting surface activity. In this aspect, the combination with spinel oxides (Mn_3O_4, Co_3O_4, Fe_3O_4, etc.) is quite promising, because their structural similarity to hexaaluminates might bring about strong interactions at the interface.

2.1. *Preparation and crystal structure of spinel/hexaaluminate*

Hexaaluminates ($Ba_{0.75}MAl_{10}O_{17.25}$, M = Al or Mn) were prepared by hydrolysis of alkoxides and subsequent calcination at 1100°C as described previously [3]. The air oxidation process [9–12] was adopted for the preparation of the composite between spinel Mn_3O_4 and hexaaluminates. Hexaaluminate powders and manganese(II) nitrate were added to ion-exchanged water which was deoxidized by N_2 bubbling overnight. The resultant suspension was vigorously stirred under N_2 atmosphere and was followed by air oxidation, which was performed by passing air bubbles through the solution at 70°C and pH ca.7. The spinel formation in the air oxidation process results from the following reaction;

$$2MnOH^{2+} + MnOH^{+} + OH^{-} \rightarrow Mn^{2+}Mn_2^{3+}O_4 + 4H^{+}.$$

As-prepared 15 wt.-% Mn_3O_4/hexaaluminate sample showed no XRD pattern due to the spinel phase. Diffraction peaks of Mn_3O_4 appeared above 30 wt.-% of loading. Microstructural analysis was performed on 10 wt.-% $Mn_3O_4/Ba_{0.75}MnAl_{10}O_{17.25}$ by a transmission electron microscope (JEOL 2000FX, HVEM Laboratory at Kyushu University). Electron diffraction showed no significant deviation of the crystal structure but the presence of isolated Mn_3O_4 particles. However, structural image (Fig. 4) in the vicinity of the basal plane surface of hexaaluminate facets (incident beam normal to (120)) apparently showed the appearance of surface layers after the air oxidation process. The thickness of this surface layer is about 4 nm. While the image of hexaaluminate is characterized by an array of 1 nm-thick layers along [001], the surface layer contains no contours corresponding to the layer structure. Since the same structural image can be retained after calcination, this surface layer is believed to consist of Mn_3O_4 with spinel structure. This was confirmed by XPS measurement, which showed the Mn $2p_{3/2}$ peak with the binding energy corresponding to Mn_3O_4.

2.2. *Surface structure of spinel/hexaaluminate*

Surface coverage of hexaaluminate microcrystals by spinel layers was studied by using chemisorption of carbon dioxide onto Ba with strong basic character [13]. Adsorption was carried out in a conventional volumetric vacuum system at room temperature. After evacuating the sample at 500°C, incremental CO_2 uptake at increasing pressures was measured with a pressure sensor. After evacuation for 1 h, the CO_2 adsorption measurement was repeated. The irreversible CO_2 chemisorption is determined from the difference of a pair of adsorption isotherms and plotted as a function of loading amount of Mn_3O_4 in Fig. 5.

The amount of CO_2 chemisorption steeply decreased with increasing the Mn_3O_4 loading, being negligible above 3 wt.-%. The CO_2 chemisorption appears to take place predominantly onto Ba species on the surface of hexaaluminate microcrystals but negligibly on Mn_3O_4. Thus, the amount of CO_2 chemisorption reflects the surface coverage by the Mn_3O_4 layer. Although the surface distribution of Ba ions on hexaaluminates is not clear, we assume that they should be exposed mainly on the basal plane of the facet which is just parallel to the monolayer including Ba. The result explains that the Mn_3O_4 layer completely covered, at least, the basal plane of hexaaluminate facets. The CO_2 adsorption remained almost zero even after heating at 700°C.

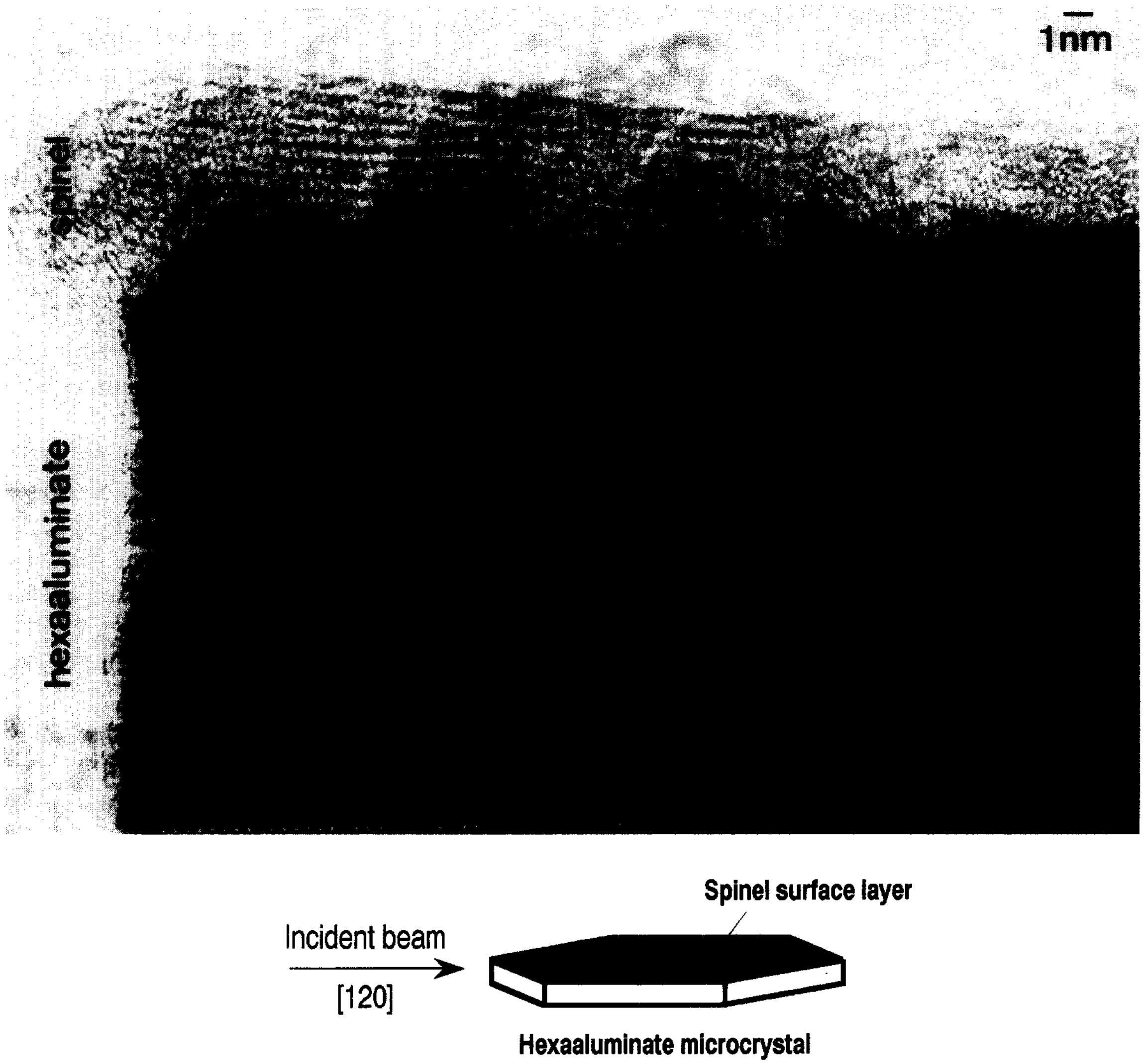

Fig. 4. TEM image of 10 wt.-% Mn_3O_4/hexaaluminate taken with an incident beam normal to (120) plane of hexaaluminate. Parallel contours represent layer structure of hexaaluminate along the *c* axis.

We believe that one of the reasons why such surface spinel layers form is the structural coherence between Mn_3O_4 and hexaaluminate. The projection of crystal structures (Fig. 6) shows that the ionic configuration in the spinel structure is analogous to that in the spinel blocks of hexaaluminate; they are composed of cubic close-packing of oxygen ions, of which tetrahedral and octahedral sites are partially occupied by small cations (Al and/or Mn). Therefore, the basal plane surface of hexaaluminate, being exactly parallel to the O_2 close-packing layer, can provide coherent interface with little stress. The air oxidation process seems effective in promoting the formation of this type of interface structure because it allows continuous growth of spinel lattices from a liquid phase. In constant, a substantial amount of CO_2 chemisorption was observed for Mn_3O_4/hexaaluminate prepared from a conventional evaporation-to-dryness process and subsequent calcination at 500°C (Fig. 5). This impregnated sample seems to contain insular Mn_3O_4 particles on the surface of hexaaluminate microcrystals.

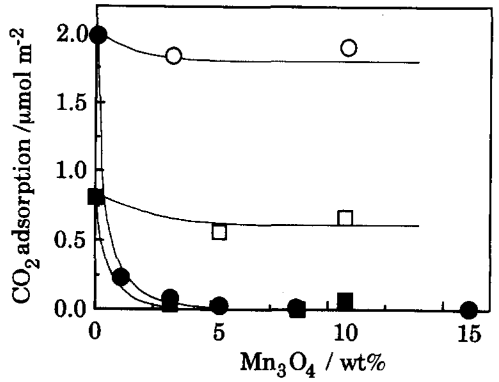

Fig. 5. Amount of irreversible CO_2 adsorption on Mn_3O_4/hexaaluminate at room temperature. ●, $Mn_3O_4/Ba_{0.75}Al_{11}O_{17.25}$ (air oxidation); ■, $Mn_3O_4/Ba_{0.75}MnAl_{10}O_{17.25}$ (air oxidation); ○, $Mn_3O_4/Ba_{0.75}Al_{11}O_{17.25}$ (evaporation to dryness); □, $Mn_3O_4/Ba_{0.75}MnAl_{10}O_{17.25}$ (evaporation to dryness).

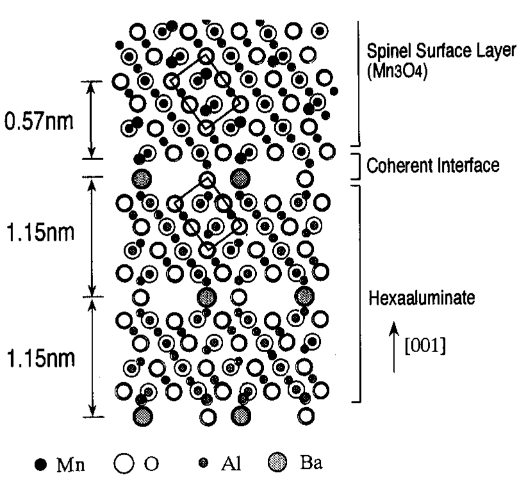

Fig. 6. Ideal interface structures of spinel/hexaaluminate.

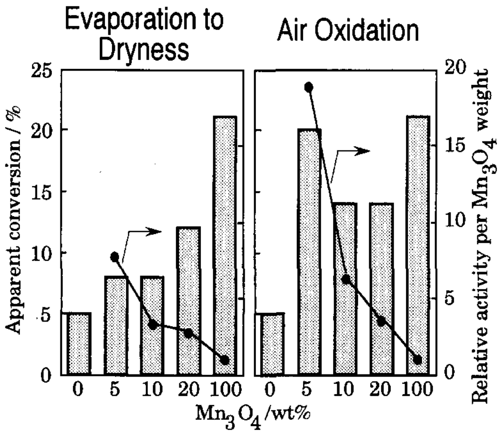

Fig. 7. Catalytic activity of $Mn_3O_4/Ba_{0.75}MnAl_{10}O_{17.25}$ for methane combustion at 400°C. $T_{10\%}$, $T_{90\%}$: temperatures at which the methane conversion into CO_2 reaches 10% and 90%, respectively. CH_4 2 vol.-%, air 98 vol.-%, $W/F = 0.01$ g min cm^{-3}.

3. Catalytic activity of surface-modified hexaaluminates for methane combustion

Catalytic activity of Mn_3O_4/hexaaluminate composites for methane oxidation was evaluated in a conventional fixed bed reactor (CH_4 2 vol.-%, air 98 vol.-%, $W/F = 0.01$ g min cm^{-3}). The methane conversion in the effluent gas was analyzed by on-line gas chromatography. The combustion activity is expressed as temperatures, $T_{10\%}$ and $T_{90\%}$, at which methane conversion of 10 and 90%, respectively, are attained.

Fig. 7 shows the apparent catalytic activity (400°C) of $Mn_3O_4/BaMnAl_{10}O_{17.25}$ prepared by air oxidation as well as conventional evaporation-to-dryness. The apparent activity of the sample from evaporation-to-dryness increased monotonously with loading amount of Mn_3O_4. This is in contrast to the air oxidation-derived sample, which retained high activity even at low loading amount. Fig. 7 also shows the specific catalytic activity per unit Mn_3O_4 loading (400°C), which is normalized by the activity of unsupported Mn_3O_4. Higher specific activity was attained for the air oxidation-derived sample at the lower amount Mn_3O_4 loading. This result is consistent with the surface microstructure of the Mn_3O_4/hexaaluminate sample. High surface coverage of hexaaluminate microcrystals by Mn_3O_4 brought about the high catalytic activity. On the other hand, the preparation by evaporation-to-dryness does not permit the high surface coverage because of the insularly dispersed structure of Mn_3O_4.

To enhance the catalytic activity of Mn_3O_4/hexaaluminate composites, the effect of partial substitution for Mn in the spinel layers was examined. The mixed spinel surface layers ($(Mn_{1-x}M_x)_3O_4$, M = Fe,Co, and Ni) were also produced on $Ba_{0.75}MnAl_{10}O_{17.25}$ by air-oxidation process. Their catalytic activities for methane combustion are summarized in Fig. 8 as a function of x in $(Mn_{1-x}M_x)_3O_4$. Co- and Ni-substitution was not effective because of incomplete coverage of the surface layer in the system. Partial substitution by Fe produced most prominent effect in promoting the catalytic activity, which reached

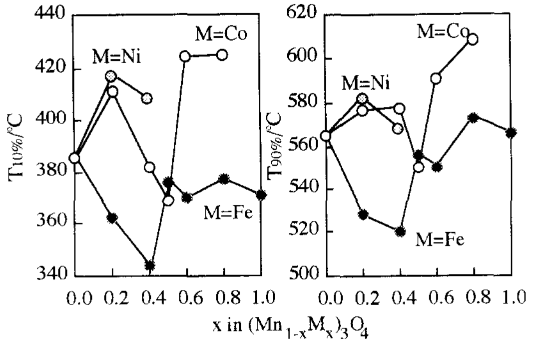

Fig. 8. Catalytic activity of 10 wt.-% $(Mn_{1-x}M_x)_3O_4/Ba_{0.75}MnAl_{10}O_{17.25}$ for methane combustion. $T_{10\%}$, $T_{90\%}$: temperatures at which the methane conversion into CO_2 reaches 10% and 90%, respectively. CH_4 2 vol.-%, air 98 vol.-%, $W/F = 0.01$ g min cm^{-3}.

the maximum at $x = 0.4$. This system produced spinel layers with complete surface coverage. Moreover, the redox property of Fe-substituted spinel surface layer is more favorable for catalytic oxidation as evident from temperature programmed desorption of O_2.

Consequently, the air oxidation process is to be expected for an excellent structural modification of hexaaluminate catalysts. This enables the almost complete coverage of hexaaluminate surface by spinel layers via formation of the coherent interface.

Acknowledgements

This study was supported by Iketani Science and Technology Foundation and The Association for the Progress of New Chemistry.

References

[1] M. Machida, K. Eguchi and H. Arai, J. Catal., 103 (1987) 385.
[2] M. Machida, K. Eguchi and H. Arai, Bull. Chem. Soc. Jpn., 61 (1987) 3659.
[3] M. Machida, K. Eguchi and H. Arai, J. Catal., 120 (1989) 386.
[4] M. Machida, K. Eguchi and H. Arai, J. Catal., 123 (1990) 477.
[5] M. Machida, K. Eguchi and H. Arai, J. Am. Ceram. Soc., 71 (1988) 1142.
[6] M. Machida, T. Shiomitsu, Y. Shimizu, K. Eguchi and H. Arai, J. Solid State Chem., 95 (1991) 220.
[7] M. Machida, T. Shiomitsu, K. Eguchi, H. Haneda and H. Arai, J. Mater. Chem., 2 (1992) 455.
[8] M. Machida, H. Inoue, T. Shiomitsu, K. Eguchi and H. Arai, Ceram. Trans. Ser., 31 (1992) 273.
[9] M. Kiyama, Bull. Chem. Soc. Jpn., 47 (1974) 1646.
[10] M. Abe and Y. Tamaura, Jpn. J. Appl. Phys., 22 (1983) L511.
[11] N. Aoki, Bull. Ceram. Soc. Jpn., 26 (1991) 195.
[12] M. Machida, A. Sato, T. Kijima and H. Arai, Chem. Lett., (1993) 1869.
[13] M. Bettman, R.E. Chase, K. Otto and W.H. Weber, J. Catal., 117 (1989) 447.